RESEARCH ARTICLE

Expression and effect of sodium-potassium-chloride cotransporter on dorsal root ganglion neurons in a rat model of chronic constriction injury

Chao-Yang Tan[1, 2, 3, #], Yan-Ping Wang[2, 4, #], Yuan-Yuan Han[1, 5, #], Bi-Han Lu[1], Wei Ji[1], Li-Cang Zhu[6], Yang Wang[1, 7], Wen-Yan Shi[1, 7], Li-Ya Shan[1, 7], Liang Zhang[1, 7], Ke-Tao Ma[1, 7], Li Li[1, 2, 7, *], Jun-Qiang Si[1, 7, 8, 9, *]

1 Department of Physiology, College of Medicine, Shihezi University, Shihezi, Xinjiang Uygur Autonomous Region, China
2 Department of Physiology, Medical College of Jiaxing University, Jiaxing, Zhejiang Province, China
3 Department of Health, Karamay Army Division, Chinese People's Liberation Army, Karamay, Xinjiang Uygur Autonomous Region, China
4 Department of Nursing, Medical College of Jiaxing University, Jiaxing, Zhejiang Province, China
5 Department of Clinical Medicine, Karamay College of Xinjiang Medical University, Karamay, Xinjiang Uygur Autonomous Region, China
6 Department of Neurosurgery, First Affiliated Hospital, College of Medicine, Shihezi University, Shihezi, Xinjiang Uygur Autonomous Region, China
7 The key Laboratory of Xinjiang Endemic and Ethnic Diseases, College of Medicine, Shihezi University, Shihezi, Xinjiang Uygur Autonomous Region, China
8 Department of Physiology, School of Basic Medical Sciences, Wuhan University, Wuhan, Hubei Province, China
9 Department of Physiology, School of Basic Medical Sciences, Huazhong University of Science and Technology, Wuhan, Hubei Province, China

Funding: *This study was supported by the National Natural Science Foundation of China, No. 30160026 (to JQS); the High Level Talent Research Project of Shihezi University of China, No. RCSX201705 (to YW).*

Graphical Abstract

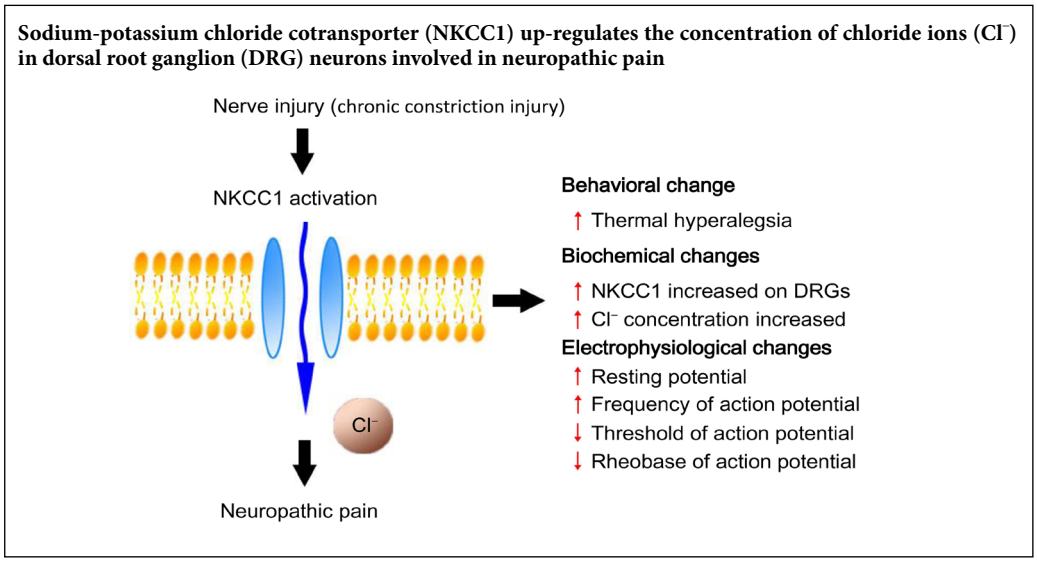

***Correspondence to:**
Jun-Qiang Si, PhD, sijunqiang@shzu.edu.cn;
Li Li, PhD, lily7588@163.com.

#These authors contributed equally to this work.

orcid:
0000-0001-6704-2115 (Jun-Qiang Si)
0000-0001-8591-0676 (Li Li)

doi: *10.4103/1673-5374.268904*

Received: *March 9, 2019*
Peer-review started: *April 13, 2019*
Accepted: *June 6, 2019*
Published online: *November 8, 2019*

Abstract

Sodium-potassium-chloride cotransporter 1 (NKCC1) and potassium-chloride cotransporter 2 (KCC2) are associated with the transmission of peripheral pain. We investigated whether the increase of NKCC1 and KCC2 is associated with peripheral pain transmission in dorsal root ganglion neurons. To this aim, rats with persistent hyperalgesia were randomly divided into four groups. Rats in the control group received no treatment, and the rat sciatic nerve was only exposed in the sham group. Rats in the chronic constriction injury group were established into chronic constriction injury models by ligating sciatic nerve and rats were given bumetanide, an inhibitor of NKCC1, based on chronic constriction injury modeling in the chronic constriction injury + bumetanide group. In the experiment measuring thermal withdrawal latency, bumetanide (15 mg/kg) was intravenously administered. In the patch clamp experiment, bumetanide (10 μg/μL) and acutely isolated dorsal root ganglion neurons (on day 14) were incubated for 1 hour, or bumetanide (5 μg/μL) was intrathecally injected. The Hargreaves test was conducted to detect changes in thermal hyperalgesia in rats. We found that the thermal withdrawal latency of rats was significantly decreased on days 7, 14, and 21 after model establishment. After intravenous injection of bumetanide, the reduction in thermal retraction latency caused by model establishment was significantly inhibited. Immunohistochemistry and western blot assay results revealed that the immune response and protein expression of NKCC1 in dorsal root ganglion neurons of the chronic constriction injury group increased significantly on days 7, 14, and 21 after model establishment. No immune response or protein expression of KCC2 was observed in dorsal root ganglion neurons before and after model establishment. The Cl^- (chloride ion) fluorescent probe technique was used to evaluate the change of Cl^- concentration in dorsal root ganglion neurons of chronic constriction injury model rats. We found that the relative optical density of N-(ethoxycarbonylmethyl)-6-methoxyquinolinium bromide (a Cl^- fluorescent probe whose fluorescence

intensity decreases as Cl^- concentration increases) in the dorsal root ganglion neurons of the chronic constriction injury group was significantly decreased on days 7 and 14 after model establishment. The whole-cell patch clamp technique revealed that the resting potential and action potential frequency of dorsal root ganglion neurons increased, and the threshold and rheobase of action potentials decreased in the chronic constriction injury group on day 14 after model establishment. After bumetanide administration, the above indicators were significantly suppressed. These results confirm that CCI can induce abnormal overexpression of NKCC1, thereby increasing the Cl^- concentration in dorsal root ganglion neurons; this then enhances the excitability of dorsal root ganglion neurons and ultimately promotes hyperalgesia and allodynia. In addition, bumetanide can achieve analgesic effects. All experiments were approved by the Institutional Ethics Review Board at the First Affiliated Hospital, College of Medicine, Shihezi University, China on February 22, 2017 (approval No. A2017-169-01).

Key Words: *bumetanide; chronic constriction injury; dorsal root ganglion; dorsal root reflex; hyperalgesia; KCC2; nerve regeneration; neuropathic pain; NKCC1; primary afferent depolarization; whole-cell patch clamp*

Chinese Library Classification No. *R446; R363;R364*

Introduction

Neuropathic pain refers to the pain caused by injury or illness of the somatosensory nervous system. Neuropathic pain has a high incidence of approximately 7%, and imposes a significant burden on individuals and society. Neuropathic pain is characterized by a complex and diverse pathological process, and variable clinical manifestations that involve different parts of the nervous system (Bruna and Velasco, 2018; Lamas and Fernández-Fernández, 2019). Peripheral nerve injury-induced neuropathic pain symptoms, such as hyperalgesia and allodynia, are associated with increased excitability in the peripheral and central nervous systems (Coull et al., 2003; Wang and Li, 2019); this increased excitability results from enhanced synaptic excitation, decreased synaptic inhibition, and increased neuronal responsiveness (Price et al., 2009). Therefore, it is of great clinical significance to study the pathogenesis of neuropathic pain and develop analgesics with a better efficacy and fewer side effects.

The sodium-potassium-chloride transporter (Na^+-K^+-$2Cl^-$ cotransporter, NKCC1) and potassium-chloride cotransporter 2 (K^+-Cl^- cotransporter, KCC2) belong to the cation-Cl^- cotransporter family. NKCC1, which is expressed in almost all secretory epithelia (Plotkin et al., 1997), maintains the concentration of Cl^- ($[Cl^-]_i$) above the electrochemical equilibrium. In contrast to NKCC1, KCC2 has a unique neuronal distribution. KCC2 is mainly expressed in central neurons, as well as in peripheral neurons of immature mammals, and is hardly expressed in peripheral neurons of adult mammals (Payne et al., 1996). NKCC1 is an inward cotransporter of Cl^- ions and is driven by sodium and potassium concentration gradients, whereas KCC2 is an inward cotransporter of Cl^- ions driven by the potassium concentration gradient. This suggests that these two transporters perform opposite regulation functions in Cl^- ion transport (Payne et al., 2003).

Some evidence has suggested that NKCC1 and KCC2 are strongly associated with neuropathic pain. For example, Hasbargen et al. (2010) found that an altered function of NKCC1 and KCC2 may contribute to the induction and maintenance of chronic neuropathic pain following spinal cord injury. The disruption of intracellular chloride homeostasis in dorsal root ganglion (DRG) neurons, which is mainly controlled by NKCC1 and neuron-specific KCC2, is related to plastic changes in sensory pathways (Price et al., 2005). One study also reported that the threshold value of harmful stimuli in NKCC1 knockout animals increased during hot-plate experiments (Sung et al., 2000). Therefore, NKCC1 and KCC2 may be involved in the production and maintenance of neuropathic pain.

Neuropathic pain caused by altered function of NKCC1/KCC2 may be associated with GABA. Previous studies have indicated that the balance between NKCC1 and KCC2 cotransporters is critical for gamma-aminobutyric acid (GABA) ergic and glycinergic responses and proper neuronal signaling (Walcott and Langdon, 2002; Payne et al., 2003). Immature visual cortex neurons and peripheral primary sensory neurons (DRG neurons and trigeminal ganglion neurons) maintain a high intracellular Cl^- concentration due to high NKCC1 expression and low (or no) KCC2 expression; these neurons exhibit shunting inhibition and membrane depolarization upon activation of GABAA receptors (Delpire, 2000; Payne et al., 2003; Li et al., 2015). At maturity, KCC2 is upregulated, and/or NKCC1 is downregulated to maintain low intracellular Cl^- concentrations, which results in GABAergic inhibitory responses. However, adult neurons can elevate intracellular Cl^- during injury, leading to a positive shift in the Cl^- equilibrium; as a result, the response to GABA becomes less hyperpolarizing or becomes excitatory, and the normal inhibitory action of GABA is altered (Rivera et al., 1999; Ikeda et al., 2003; Payne et al., 2003). These results suggest that severe injury of the peripheral nerve may shift the GABA action towards an excitatory state by modulating NKCC1 and/or KCC2, thereby contributing to hyperexcitability and maintaining chronic pain (Miletic and Miletic, 2008; Janssen et al., 2011).

However, the relationship between NKCC1/KCC2 and maintenance of neuropathic pain after chronic constriction injury (CCI) injury has not been elucidated. Thus, the present study investigated the increased expression of NKCC1 and KCC2 in DRG neurons after CCI modeling (Bennett and Xie, 1988). This resulted in an increased Cl^- concentration in DRG neurons, which in turn enhanced GABA-mediated primary afferent depolarization and induced the dorsal root reflex response. Eventually, the excitability of DRG neurons was enhanced, which resulted in the production of neuropathic pain.

Materials and Methods

Experimental animals and groups

A total of 145 male Sprague-Dawley rats aged 8–12 weeks and weighing 200–250 g were provided by Animal Cen-

ter, Xinjiang Medical University, China (license No. SCXK (Xin) 2003-0001). The rats were randomly divided into four groups. The control group comprised 40 rats (thermal withdrawal latency, TWL, 5 rats; immunohistochemistry, 10 rats; western blot assay, 10 rats; N-(ethoxycarbonylmethyl)-6-methoxyquinolinium bromide, MQAE, 10 rats; and patch clamp, 5 rats). The sham group comprised 10 rats (TWL, 5 rats; and patch clamp, 5 rats). The rat sciatic nerve was exposed in the sham group without ligation. The CCI group, which was verified based on TWL, included 85 rats (TWL, 5 rats; immunohistochemistry, 15 rats, day 7, day 14, and day 21, 5 rats each; western blot assay, 30 rats, day 7, day 14, and day 21, 10 rats each; MQAE, 20 rats, day –1, day 7, day 14, and day 21, 5 rats each; and patch clamp 15 rats, day 7, day 14, and day 21, 5 rats each). Rats in the CCI group were subjected to CCI and given the same dose of vehicle as the CCI + bumetanide group. The CCI + bumetanide group, consisted of 10 rats (TWL, 5 rats; and patch clamp, 5 rats). Rats in the CCI + bumetanide group were injected with bumetanide (see drug administration for details). All experiments were conducted in accordance with approval from the Institutional Ethics Review Board at the First Affiliated Hospital, College of Medicine, Shihezi University, China on February 22, 2017 (approval No. A2017-169-01). The experimental procedure followed the United States National Institutes of Health Guide for the Care and Use of Laboratory Animals (NIH Publication No. 85-23, revised 1996).

Preparation of the CCI models

Rats were intraperitoneally anesthetized with 1% pentobarbital sodium (50 mg/kg). The sciatic nerve trunk was exposed using the method proposed by Bennett and Xie (1988). In the proximal 5 mm of the sciatic nerve comprising three nerve bifurcation fibers, 4-0 chromic sheep gut was used for ligation with four laps of the sciatic nerve, using a spacing of 1 mm per lap. This ligation strength caused a mild tremor in the calf muscle but had no effect on the blood transport in the nerve trunk. After surgery, the rats were exposed to single-cage feeding, enhanced animal nutrition, and a strict 12-hour light/dark cycle. Cages for feeding the rats were cleaned and disinfected every two days. In the sham group, the sciatic nerve was exposed but not ligated. If the withdrawal time of the hind limbs on the surgery side of the rats on day 7 decreased by > 30% compared with that in the preoperative test, the CCI model preparation was considered successful.

Drug administration

Bumetanide (15 mg/kg; Apexbio, Houston, TX, USA), an inhibitor of NKCC1, was intravenously injected into the tail of animals in the CCI + bumetanide group once a day for 30 minutes before the measurement of rat TWL, from preoperative day 1 to postoperative day 21. Rats in the CCI group were injected with the same dose of dimethyl sulfoxide (0.1%). In the patch clamp experiment, bumetanide was incubated (10 μg/μL) with acutely dissociated DRG neurons (modeling for 14 days) for 1 hour or intrathecally injected (5 μg/μL) into the animals once a day, from preoperative day 1 to postoperative day 14. In the CCI group, 0.08% dimethyl sulfoxide was incubated with acutely dissociated DRG neurons (modeling for 14 days) for 1 hour or intrathecally injected (0.04%) into the animals once a day, from preoperative day 1 to postoperative days 14.

The Hargreaves Test

Thermal hyperalgesia was assessed according to a previous protocol (Wang et al., 2017). An automatic thermal radiation stimulator (UGO BASILE 37370 Plantar Test Apparatus, Italy) was used at a fixed time (18:00–20:00 each day) and at the same laboratory. Each rat was placed in the plastic box and was given thermal stimulation according to established procedures. TWL was defined as the duration from onset of application of thermal stimulation to withdraw of either hind-paw. Each rat was tested three times at intervals of 5 minutes, and the average of three tests was obtained. Animals in all groups were tested at –1, 1, 3, 7, 14 and 21 days.

Immunohistochemistry (paraffin-embedded sections)

Tissue specimens were collected from the four groups on preoperative day 1 and postoperative days 7, 14, and 21. Rats were sacrificed at the day before surgery and at the postoperative days 7, 14, and 21. Rats in all groups were intraperitoneally anesthetized with 1% pentobarbital sodium 50 mg/kg. Then, 4% paraformaldehyde was used for cardiac perfusion. After preliminary fixation of the animal tissues, the spinal canal was cut to expose and strip the spinal cord. The surgery side and contralateral L4–6 spinal cord segmental DRG neurons connected to the sciatic nerve were immediately removed. The specimens were fixed with 4% polyformaldehyde for 48 hours. The DRG samples were embedded in paraffin in axial continuous sections (slice thickness, 3.5 μm). After dewaxing, the paraffin sections were repaired, blocked with endogenous peroxidase, washed with phosphate buffered saline, and incubated with the rabbit anti-NKCC1 (Cell Signaling Company, Danfoss Town, Boston, MA USA) polyclonal antibody (1:500) or rat anti-KCC2 (Abcam, Cambridge, UK) monoclonal antibody (1:500) at 4°C overnight. Subsequently, the samples were incubated with goat anti-rabbit lgG (1:10,000) at 37°C for 1 hour, stained with a 3,3′-diaminobenzidine chromogenic kit, counterstained, dehydrated, and sealed. A standard optical microscope (Olympus, Tokyo, Japan) was used to observe the tissue cells and to capture images. The exocrine adenocytes of rat pancreatic tissues served as the positive control for NKCC1, and neurons in the rat CA1 hippocampus were used as a positive control for KCC2.

NKCC1-immunoreactive cells (stained brown-yellow) were counted under a microscope (Olympus). For each count, histochemical sections were selected on preoperative day 1 (the control group) and postoperative days 7, 14, and 21. DRG neurons were classified into three types according to diameter size, as follows: Large neurons (diameter larger than 40 μm), medium-sized neurons (diameter of 20–40 μm), and small neurons (diameter less than 20 μm). Three fields of view were selected for each slice, the three fields of

view were counted respectively, and the average value was taken as an evaluation index.

Western blot assay

The tissue specimens for western blot assay were collected from each group on preoperative day 1 and postoperative days 7, 14, and 21. The animals were sacrificed by decapitation, with immediate stripping of the connected sciatic nerve on the surgery side and contralateral L_{4-6} DRG organization. The proteins were extracted, subjected to sodium dodecyl sulfate polyacrylamide gel electrophoresis, and transferred to a wet membrane film. Membranes were incubated with the rabbit anti-NKCC1 polyclonal antibody (1:1000; Cell Signaling Company, Danfoss Town, Boston, MA, USA), rat anti-KCC2 monoclonal antibody (1:1000; Abcam, Cambridge, UK), or rabbit anti-GAPDH (1:1000) at 4°C overnight, and with goat anti-rabbit lgG (1:10,000; Sugisuke Bridge, Beijing, China) or goat anti-rat lgG (1:10,000; Sugisuke Bridge) at room temperature. The membranes were stained using an ECL chromogenic kit. Images of the samples were captured and analyzed by Image-Pro Plus 6.0 software (Media Cybernetics, Rockville, MD, USA). The ratio was calculated between the gray value of NKCC1 (or KCC2) and the gray value of GAPDH. This ratio was used to reflect the relative expression of NKCC1 or KCC2.

Cl^- fluorescence probe (MQAE)

The L4–6 DRG specimens were collected from each group on preoperative day 1 and postoperative days 7, 14, and 21. According to the experimental procedure of Batti et al. (2013), the animals were sacrificed by decapitation, with immediate stripping of the sciatic nerve on the surgery side and contralateral L4–6 DRG organization. The samples were cut with eye scissors, subjected to enzyme digestion, and centrifuged. After removal of the clear liquid, the specimens were placed on a 24-well plate. MQAE buffer was added and incubated at 37°C, and specimens were then cleaned with a buffer. Quenching drops were prevented, and a fluorescence microscope was used to record fluorescence intensity. When the concentration of Cl^- in the cell increased, the fluorescence intensity of MQAE was proportionally reduced. Fluorescence intensity was analyzed using CellSens Standard Image Acquisition software and Image Pro Plus 6.0 software (Media Cybernetics).

Acute separation of DRG neurons

On postoperative day 7, rats were sacrificed by cervical dislocation and the segmental L4–6 DRG was quickly removed. The redundant nerve fibers and connective tissues were trimmed, and the DRG was treated with digestive enzymes (pancreatic protease, 0.12 mg/mL; Sigma, St. Louis, MO, USA; collagen enzyme, 0.1 mg/mL, Sigma) in Dulbecco's modified Eagle's medium at 37°C for 30 minutes. A suitable amount of digestive enzyme inhibitors was then added to terminate digestion, and centrifugation was performed at 1000 r/min for 5 minutes. The supernatant was removed, and extracellular fluid, containing NaCl, 150 mM; KCl, 5 mM; $CaCl_2$, 2.5 mM; $MgCl_2$, 1 mM; HEPES, 10 mM; and D-glucose 10 mM at pH 7.4, was added to the cells and left to stand. The osmotic pressure of the solution was 340 mOsm, and electrophysiological experiments were performed after the cells had adhered to the bottom of the dish.

Patch clamp recording

DRG neurons comprised three types: Large cells with diameters larger than 40 μm, small cells with diameters less than 20 μm, and medium-sized cells with diameters between 20 and 40 μm (Rau et al., 2005). The experiment was conducted at a constant temperature of 22.0 ± 2.0°C. An Axon 700B amplifier was used to record the results of the action potential. The glass microelectrode control resistance was 2–5 MΩ. The fluid in the filling electrode comprised the following (mM): KCl, 140; $CaCl_2$, 1; $MgCl_2$, 2; HEPES, 10; and egtazic acid. The results showed complete cell structure, clear cell nuclei, and desirable refractive performance. Small- and medium-sized cells with diameters of less than 40 μm were used to record the results of the action potential. To achieve high-resistance sealing in whole-cell voltage clamp mode, after the membrane had been broken, the whole-cell voltage clamp mode was switched to the current clamp mode, and ramp stimulation (duration, 1000 ms; amplitude range, 0–500 pA) was performed. Action potentials were recorded. The resting potential was recorded in the absence of input current after conversion to the current clamp mode. The action potential threshold is the membrane potential of the stimulated cell that initiates an action potential, and can reflect the degree of difficulty of evoking action potentials in stimulated cells. The action potential frequency denotes the number of action potentials of stimulated cells per second. The difference between the resting potential and threshold potential represents the difficulty of inducing an action potential after cell stimulation. Stepwise increments in stimulation (from 0 pA to 600 pA in 50-pA increments with a pulse duration of 150 ms) were performed to determine the rheobase, then another phase of stimulation (duration, 500 ms; amplitude, twice the strength of the rheobase) was performed to record the number of action potentials. The recorded electrical signals were amplified using a MultiClamp 700B amplifier (Molecular Devices, LLC, Sunnyvale, CA, USA), filtered at 10 kHz, and converted into digital signals by an Axon Digidata 1550A D/A converter (Molecular Devices, LLC) at a sampling frequency of 10 to 20 kHz.

Statistical analysis

The experimental data are presented as the mean ± standard error of the mean. SPSS 17.0 software (SPSS Inc., Chicago, IL, USA) was used for all statistical analyses. Two-group comparisons were conducted using independent-sample *t*-test. Comparison of three or more groups using one-way analysis of variance and Tukey's *post hoc* test was used to compare differences between more than two groups. $P < 0.05$ was considered as statistically significant.

Results

Behavioral differences

The rats in each group were observed to have good health, with smooth and clean body fur. After surgery, rats from the CCI group licked their feet and swung the hind limb on the surgical side. The hind limb on the surgical side failed to carry weight, and the rat paws exhibited adduction and slight evagination. Limping was notable, and frequent licking and retractions were observed. No remarkable behavioral changes or movement disorders were observed in the sham group. No self-biting occurred after surgery in the CCI group.

Between-group differences in TWL

TWL of the hind limb of the surgical side was significantly shorter in the CCI group than in the control group at all time points (n = 5, $P < 0.05$). The TWL values in the CCI group were significantly lower than those in the sham group on postoperative days 7, 14, and 21. The TWL values in the CCI + bumetanide group were significantly higher than those of the CCI group on postoperative days 7, 14, and 21. No significant difference in TWL was observed between sham group and the other groups on postoperative days 1 and 3. No significant difference in TWL was detected between the sham group and the control group at all time points. The TWL of the CCI group was significantly shorter on postoperative days 7, 14, and 21 than those on preoperative day 1 (**Figure 1**).

Expression levels of NKCC1 and KCC2 in rat DRG neurons

For normal control rats, acinar cells in the pancreatic exocrine section were used as the positive control for NKCC1 expression. Under the microscope, the cell membrane of the visible glandular cells exhibited specific shading and a light brown-yellow color (**Figure 2A**), which represents the expression of NKCC1. The rat DRG neurons showed the same specificity, which indicates that NKCC1 was positively expressed in the DRG neurons (**Figure 2B**). Hippocampal CA1 neurons were used as the positive control for KCC2 expression. Neurons in the visible hippocampus CA1 area showed membrane-specific staining and appeared light yellow under optical microscopy (**Figure 2F**). The same specific color was not observed in the DRG neuronal membrane of the rats, which indicates that KCC2 was not expressed in the DRG neuronal membrane (**Figure 2G**).

In the CCI group, the same acinar cells in the pancreatic exocrine section were used as the positive control for NKCC1. Specific staining for NKCC1 expression was performed on the DRG neuronal membrane of the rats in the CCI group on postoperative days 7, 14, and 21 (**Figure 2C–E**). The intensity was markedly greater in the CCI group than in the control group. In the hippocampal CA1 neurons of CCI rats, the KCC2-immunoreactive control was not detected on postoperative days 7, 14, or 21. Specific staining of the DRG neuronal membrane revealed no expression of KCC2 (**Figure 2H–L**). **Figure 2K** shows that the grayscale value of NKCC1-immunoreactive cells among DRG neurons on postoperative days 7, 14, and 21 was significantly higher than that of the control group (n = 6).

NKCC1-positive cell count

The number of large, medium, and small NKCC1-positive cells (stained brown yellow) in total 1000 DRG neurons on the surgical side on preoperative day 1 and postoperative days 7, 14, and 21 was counted. The standards for counting comprised complete cell structure, clear nuclear membrane, and presence of cells with positive NKCC1 expression. As shown in **Figure 3**, preoperative NKCC1-immunoreactive neurons were mainly composed of medium-sized cells. Compared with the control group (n^+ = 41), the number of medium-sized cells significantly increased on postoperative day 7 (n^+ = 87, n = 1000, $P < 0.01$) and further increased on postoperative day 14 (n^+ = 81, n = 1000, $P < 0.01$) and 21 (n^+ = 83, n = 1000, $P < 0.01$). Compared with the control group (n^+ = 22, n = 1000, $P < 0.01$), the small NKCC1-positive cells in the DRG also significantly increased on postoperative day 14 (n^+ = 58, n = 1000, $P < 0.01$). No significant difference was detected in the number of large NKCC1-positive cells before (n^+ = 20, n = 1000, $P < 0.01$) and after CCI surgery at day 7 (n^+ = 38, n = 1000, $P < 0.01$), day 14 (n^+ = 34, n = 1000, $P < 0.01$), and day 21 (n^+ = 30, n = 1000, $P < 0.01$).

Protein expression levels of NKCC1 and KCC2 in rat DRGs

Western blot assay results showed that NKCC1 was expressed in the DRG neurons of control rats (**Figure 4A**), whereas KCC2 was not (**Figure 4B**). **Figure 5** shows that NKCC1 protein was expressed in DRG neurons in the control group on postoperative days 7, 14, and 21 (**Figure 5A**). Densitometry analysis showed that NKCC1 protein expression significantly increased on postoperative days 14 and 21 ($P < 0.01$, n = 6; **Figure 5B**).

Detection of chloride concentration changes in DRG neurons using a Cl^- fluorescence probe

A Cl^- fluorescence probe (MQAE) was used to detect the concentration of intracellular Cl^- in the DRG neurons. The intensity of blue fluorescence was inversely proportional to the concentration of Cl^- in the DRG neurons. The experiment evaluated the changes in the intracellular Cl^- concentration of the segmental L4–6 DRG neurons on the surgical side in the control and CCI groups (**Figure 6A**). The concentration of Cl^- in the DRG neurons of the CCI group was significantly higher than those of the control group on postoperative days 7 and 14 (**Figure 6A** and **B**). However, no significant difference in the intracellular Cl^- concentration was observed in the DRG neurons of the CCI and control groups on postoperative day 21 (**Figure 6A** and **B**).

Changes in action potentials

Changes in action potentials in the small- and medium-sized DRG neurons of the CCI and control groups were evaluated. Oblique wave stimulation (1000 ms, 1000 pA) was applied to the DRG neurons; this caused cell membrane polarization

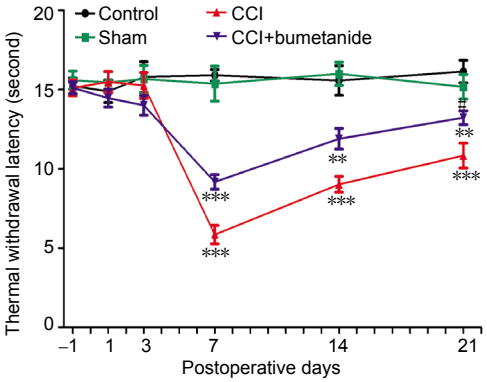

Figure 1 Bumetanide attenuates CCI-induced hyperalgesia.
Compared with the control group, thermal withdrawal latency values significantly decreased within the CCI group. Each rat was tested three times at intervals of 5 minutes. $**P < 0.01$, $***P < 0.001$, *vs.* control group; $\#P < 0.05$, $\#\#P < 0.01$, *vs.* CCI group. Data are expressed as the mean ± SEM ($n = 5$; one-way analysis of variance followed by Tukey's *post hoc* test). CCI: Chronic constriction injury.

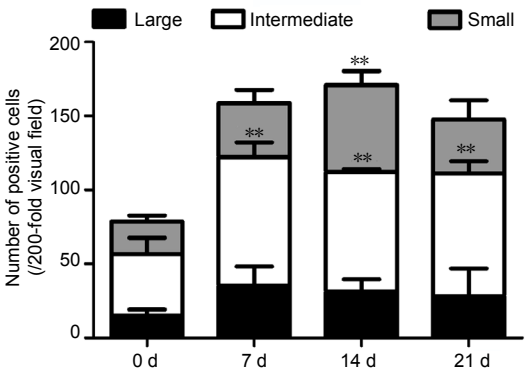

Figure 3 NKCC1-immunoreactive cell count in dorsal root ganglion neurons.
Compared with the control group ($n^+ = 41$), the number of medium-sized cells on postoperative days 7 ($n^+ = 87$), 14 ($n+ = 81$), and 21 ($n^+ = 83$) significantly increased ($n^+ = 292$, $n^- = 3708$). Compared with the control group ($n^+ = 22$), the number of small cells on postoperative day 14 ($n^+ = 58$) significantly increased ($n^+ = 80$, $n^- = 1920$). $**P < 0.01$, *vs.* control group (0 day). Data are expressed as the mean ± SEM (one-way analysis of variance followed by Tukey's *post hoc* test). NKCC1: Na^+-K^+-$2Cl^-$ cotransporter. n^+: positive cells; n^-: negative cells.

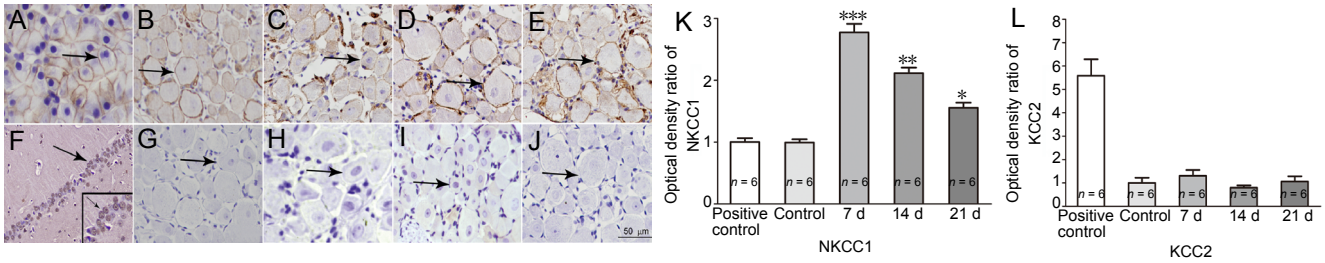

Figure 2 Immunoreactivity of NKCC1 and KCC2 in DRG and hippocampal CA1 neurons.
(A) Positive control for NKCC1 (acinar cells of the outer secreting portion of rat pancreatic tissue). (B) DRG neurons of rat (NKCC1-positive). (C–E) DRG neurons of CCI models on postoperative days 7, 14, and 21 (NKCC1-positive). (F) Positive control for KCC2 (CA1 neurons in the rat hippocampus). (G) DRG neurons of rats (KCC2-negative, brownish yellow represents NKCC1expression). (H–J) DRG neurons of CCI models on postoperative days 7, 14, and 21 (KCC2-negative) (original magnification, 400×). Black arrows indicate immunohistochemically positive cells. Brownish yellow indicates positive expression of NKCC1 or KCC2. No brownish yellow indicates negative expression of KCC1 or KCC2. Scale bar: 50 μm. (K, L) Histogram of the grayscale values of NKCC1 and KCC2 immunohistochemically positive cells. $*P < 0.05$, $**P < 0.01$, $***P < 0.001$, *vs.* control group. Data are expressed as the mean ± SEM ($n = 6$; one-way analysis of variance followed by Tukey's *post hoc* test). CCI: Chronic constriction injury; DRG: dorsal root ganglion; KCC2: K^+-Cl^--cotransporter; NKCC1: Na^+-K^+-$2Cl^-$ cotransporter.

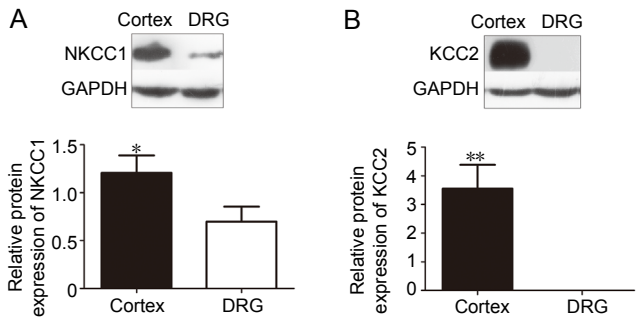

Figure 4 Protein expression levels of NKCC1 and KCC2 in DRG neurons.
(A) Positive control group (cortex cells) of NKCC1 compared with the DRG neurons group. (B) Positive control group (cortex cells) of KCC2 compared with the DRG neurons group. $*P < 0.05$, $**P < 0.01$, *vs.* DRG group. Data are expressed as the mean ± SEM ($n = 6$; independent-sample *t*-test). NKCC1: Na^+-K^+-$2Cl^-$ cotransporter; KCC2: K^+-Cl^--cotransporter; DRG: dorsal root ganglion.

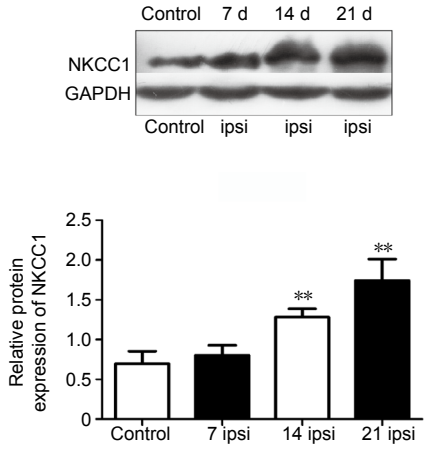

Figure 5 NKCC1 protein expression in dorsal root ganglion neurons of chronic constriction injury models after 7, 14, and 21 days.
Surgery side (ipsi) on postoperative day 14 compared with the control group. $**P < 0.01$, *vs.* control group. Data are expressed as the mean ± SEM ($n = 6$; one-way analysis of variance followed by Tukey's *post hoc* test). NKCC1: Na^+-K^+-$2Cl^-$ cotransporter; ipsi: ipsilateral.

to reach the threshold level and evoked an action potential. Different traces of action potential were detected (**Figure 7A**). **Figure 7B** shows that the resting potential of small and medium DRG neurons was significantly lower in the CCI group than in the control group ($P < 0.05$). **Figure 7B** shows that the action potential threshold of the CCI group was not significantly different to that of the control group ($P > 0.05$). The action potential frequency of the DRG neurons was significantly higher in the CCI group than in the control group ($P < 0.01$). The difference between the resting potential and threshold potential of the DRG neurons was significantly smaller in the CCI group than in the control group ($P < 0.01$). Treatment with 3×10^{-4} M bumetanide effectively reversed the changes in action potentials of DRG neurons in CCI rats (**Figures 8** and **9**).

Discussion

Nearly all DRG neurons express NKCC1 (Sung et al., 2000). MQAE analysis (Zheng et al., 2007) has indicated that, due to the presence of NKCC1, the concentration of Cl^- in DRG neurons was three to four times higher than that at baseline. KCC2 has been reported to be expressed centrally and to contribute to the low intracellular Cl concentration and the maintenance of GABAergic inhibitory responses (Coull et al., 2003). However, NKCC1 has been present in afferent neurons and increased the intracellular Cl^- concentration, thereby facilitating primary afferent depolarization and presynaptic inhibition in DRG neurons. Researchers have disputed whether KCC2 is expressed in neurons in the peripheral nervous system. Funk et al. (2008) claimed that KCC2 is expressed in DRG neurons, whereas others have found no evidence of this (Gagnon et al., 2013). In the present study, we found that NKCC1 was expressed in the normal rat DRG neuronal membrane, whereas KCC2 was absent in DRG neurons. Owing to the absence of KCC2 expression in DRG neurons, the Cl^- concentration remained higher than the extracellular concentration (Price et al., 2005, 2009; Hasbargen et al., 2010; Munro et al., 2011). Taken together, our results indicate that rat DRG neurons contain NKCC1 but not KCC2.

Previous studies have reported the relevance of early disruption of NKCC1 and KCC2 expression in the development of secondary allodynia and hyperalgesia (Coull et al., 2003; Morales-Aza et al., 2004; Price et al., 2005, 2009; Funk et al., 2008; Delpire and Austin, 2010). The results of bumetanide administration revealed that blocking NKCC1 activity following spinal cord injury and sciatic nerve lesion reduced hyperalgesic responses at the early stages (Modol et al., 2014). Consistent with the present results, previous studies have reported that NKCC1 knockout mice exhibit a loss of sensitivity to thermal stimulation (Sung et al., 2000), which further indicates that NKCC1 upregulation after nerve injury participates in the modulation of pain thresholds. In the present study, both immunohistochemistry and Western-Blot results indicated that the expression of NKCC1 increased significantly after CCI modeling. In addition, the TWL of rats was significantly reduced after CCI, and these changes were partially inhibited after the application of bumetanide (a blocker of NKCC1). However, we did not observe pain-like behaviors in the CCI group on days 1 and 3, which is not consistent with a previous study that reported pain-like behaviors in the CCI group on day 3 but not day 1 (Abbaszadeh et al., 2018). We think this difference is related to the tightness of the 4-0 chromium sheep gut. In summary, the increased expression of NKCC1 was closely related to the production of neuropathic pain.

NKCC1 expression increased to abnormal levels in the small- and medium-sized DRG neurons, and this result was associated with pain. Moreover, research has shown that small- and medium-sized DRG neurons of the CCI models were more sensitive to the transmission of pain information and therefore generated peripheral sensitization (Modol, 2014). It is possible that this phenomenon could generate an excitatory postsynaptic potential that further increases the excitability of nociceptive neurons of the spinal cord dorsal horn, leading to central sensitization and increased pain sensitivity (Samuel, 2008). In our study, NKCC1 expression in small- and medium-sized DRG neurons increased, whereas KCC2 remained unexpressed. Furthermore, the concentration of Cl^- in the small- and medium-sized DRG neuronal cells also significantly increased. Our results are consistent with previous studies. In summary, the expression of NKCC1 is significantly increased in small and medium-sized DRG neurons, which is involved in the pathogenesis of neuropathic pain.

Studies have reported that increased excitability of DRG neurons is one of the main mechanisms underlying neuropathic pain (Coull et al., 2003; Price et al., 2009). The Aδ and C nerve fibers of small- and medium-sized DRG neurons transmit pain information (Trapp, 2006). In patients with cancer pain and in a rat model of chronic compression of the DRG (Jacobsen et al., 2016), the sensory projection Aδ and C nerve fibers in the spinal cord dorsal horn in the wide dynamic range were found to significantly increase their neuronal discharge, which suggests that the development of the chronic pain state is strongly associated with increased excitability of neurons. The present study found that the number of action potentials of DRG neurons was significantly higher in the CCI group than in the control group, and that the threshold level was lower in the CCI group than in the control group. This indicates that the excitation of small- and medium-sized neurons in the CCI group increased, and that the conduction ability for pain information was enhanced. Increased excitability in the DRG has been found to enhance nociceptive inputs to supraspinal sites under chronic pain conditions (Walcott and Langdon, 2002; Ismailov et al., 2004). We also found that, compared with the control group, the resting potential and the frequency of action potentials in the CCI group were increased and the threshold and rheobase of action potentials were decreased, thereby leading to the increased excitability of DRG neurons. In conclusion, increased excitability of DRG neurons mediates the development of neuropathic pain.

Altogether, our results indicate that the expression of

NKCC1 increased in small- and medium-sized DRG neurons after CCI, which led to an increase in intracellular Cl^- concentration. Therefore, with the high intracellular Cl^- concentration, regardless of the factors that open Cl^- channels in the DRG neuron cell body (such as GABA and Gly), which can be a secondary cause of the increase in intracellular Cl^- in extracellular fluid, the neuronal cell body will be depolarized. The cell body of DRG neurons will then be excited, which results in easier production of abnormal electrical activity and transmission of a stronger signal to the central nervous system (**Figure 10**).

The present study has some limitations. We did not conduct the Von Frey test, and instead used the Hargreaves test because of the available equipment in our laboratory. We used immunohistochemistry rather than immuno-staining to identify NKCC1 and KCC2, because we did not have instruments for immuno-staining in our laboratory. We will supplement these experiments in future work. In addition, previous studies have demonstrated that increased pNKCC1 signaling induced by inflammatory mediators is associated with enhanced Cl^- accumulation in DRG neurons (Funk et al., 2008). The NKCC1 protein detected in this study was non-phosphorylated, whereas the expression of phosphorylated NKCC1 in rat DRG neurons in the CCI model was not detected. This study confirmed the presence of NKCC1 in the primary sensory neurons of the CCI model and its increased expression upon the occurrence of neuropathic pain. However, the expression and effects of NKCC1 in the spinal cord, thalamus, and cerebral cortex remain unknown and should be investigated in future experiments.

In summary, our findings indicate that the modulation of NKCC1 may represent a novel therapeutic strategy for the treatment of neuropathic pain, since neuropathic pain has been linked to enhanced functional expression of NKCC1. Our findings also highlight the relevance of blocking early changes in NKCC1 activity after nerve injury to reduce hyperalgesia. Furthermore, bumetanide as a blocker of NKCC1 has the potential for analgesia. Thus, this study provides a useful theoretical basis and potential clinical application for establishing a new accurate and effective drug target for chronic pain.

Acknowledgments: *We are very grateful to the Key Laboratory of Xinjiang Endemic and Ethnic Diseases, China for providing excellent technical support.*
Author contributions: *Study conception and design: JQS, LL, KTM and LZ; experimental data analysis: WYS, LYS and LCZ; implementation of the study and writing of the manuscript: CYT, YPW and YYH; statistical expertise: BHL, WJ and YW; fundraising: JQS and YW. All authors approved the final version of the paper.*
Conflicts of interest: *The authors declare that there are no conflicts of interest associated with this manuscript.*
Financial support: *This study was supported by the National Natural Science Foundation of China, No. 30160026 (to JQS); the High Level Talent Research Project of Shihezi University of China, No. RCSX201705 (to YW). The funding sources had no role in study conception and design, data analysis or interpretation, paper writing or deciding to submit this paper for publication.*
Institutional review board statement: *All experiments were conducted in accordance with approval from the Institutional Ethics Review Board at the First Affiliated Hospital, College of Medicine, Shihezi University, China on February 22, 2017 (approval No. A2017-169-01).*
Copyright license agreement: *The Copyright License Agreement has been signed by all authors before publication.*
Data sharing statement: *Datasets analyzed during the current study are available from the corresponding author on reasonable request.*
Plagiarism check: *Checked twice by iThenticate.*
Peer review: *Externally peer reviewed.*

Open peer reviewer: *Ben Christensen, University of Utah, USA; Michele R Colonna, Universita degli Studi di Messina, Italy; Giulia Ronchi, University of Torino, Italy.*
Additional file: *Open peer review reports 1, 2 and 3.*

References

Abbaszadeh A, Darabi S, Hasanvand A, Amini-Khoei H, Abbasnezhad A, Choghakhori R, Aaliehpour A (2018) Minocycline through attenuation of oxidative stress and inflammatory response reduces the neuropathic pain in a rat model of chronic constriction injury. Iran J Basic Med Sci 21:138-144.

Batti L, Mukhtarov M, Audero E, Ivanov A, Paolicelli RC, Zurborg S, Gross C, Bregestovski P, Heppenstall PA (2013) Transgenic mouse lines for non-invasive ratiometric monitoring of intracellular chloride. Front Mol Neurosci 2013;6:11.

Bennett GJ, Xie YK (1988) A peripheral mononeuropathy in rat that produces disorders of pain sensation like those seen in man. Pain 33:87-107.

Bruna J, Velasco R (2018) Sigma-1 receptor: a new player in neuroprotection against chemotherapy-induced peripheral neuropathy. Neural Regen Res 13:775-778.

Carlton SM (2014) Nociceptive primary afferents: they have a mind of their own. J Physiol 592:3403-3411.

Coull JA, Boudreau D, Bachand K, Prescott SA, Nault F, Sik A, De Koninck P, De Koninck Y (2003) Trans-synaptic shift in anion gradient in spinal lamina I neurons as a mechanism of neuropathic pain. Nature 424:938-942.

Delpire E (2000) Cation-chloride cotransporters in neuronal communication. News Physiol Sci 15:309-312.

Delpire E, Austin TM (2010) Kinase regulation of Na^+-K^+-$2Cl^-$ cotransport in primary afferent neurons. J Physiol 588:3365-3373.

Funk K, Woitecki A, Franjic-Wurtz C, Gensch T, Mohrlen F, Frings S (2008) Modulation of chloride homeostasis by inflammatory mediators in dorsal root ganglion neurons. Mol Pain 4:32.

Gagnon M, Bergeron MJ, Lavertu G, Castonguay A, Tripathy S, Bonin RP, Perez-Sanchez J, Boudreau D, Wang B, Dumas L, Valade I, Bachand K, Jacob-Wagner M, Tardif C, Kianicka I, Isenring P, Attardo G, Coull JA, De Koninck Y (2013) Chloride extrusion enhancers as novel therapeutics for neurological diseases. Nat Med 19:1524-1528.

Hasbargen T, Ahmed MM, Miranpuri G, Li L, Kahle KT, Resnick D, Sun D (2010) Role of NKCC1 and KCC2 in the development of chronic neuropathic pain following spinal cord injury. Ann N Y Acad Sci 1198:168-172.

Ikeda M, Toyoda H, Yamada J, Okabe A, Sato K, Hotta Y, Fukuda A (2003) Differential development of cation-chloride cotransporters and Cl- homeostasis contributes to differential GABAergic actions between developing rat visual cortex and dorsal lateral geniculate nucleus. Brain Res 984:149-159.

Ismailov I, Kalikulov D, Inoue T, Friedlander MJ (2004) The kinetic profile of intracellular calcium predicts long-term potentiation and long-term depression. J Neurosci 24:9847-9861.

Jacobsen DP, Moen A, Haugen F, Gjerstad J (2016) Hyperexcitability in spinal WDR neurons following experimental disc herniation is associated with upregulation of fractalkine and its receptor in nucleus pulposus and the dorsal root ganglion. Int J Inflam 2016:6519408.

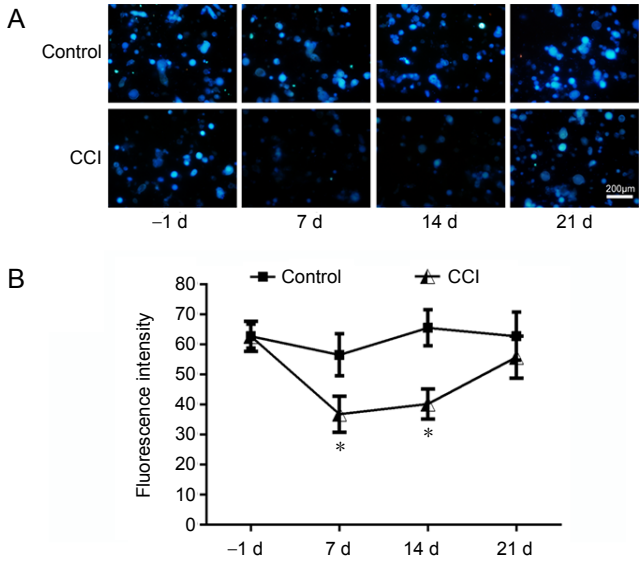

Figure 6 MQAE fluorescence intensity was inversely proportional to Cl^- concentration.
(A) Changes in the concentration of intracellular Cl^- in the dorsal root ganglion neurons of the CCI group on preoperative day 1 and on postoperative days 7, 14, and 21 were detected using MQAE. (B) Quantification of chloride fluorescence intensity in the dorsal root ganglion neurons on preoperative day 1 and on postoperative days 7, 14, and 21. *P < 0.05, *vs.* control group. Data are expressed as the mean ± SEM (n = 5; independent-sample t-test). CCI: Chronic constriction injury; MQAE: N-(ethoxycarbonylmethyl)-6-methoxyquinolinium bromide.

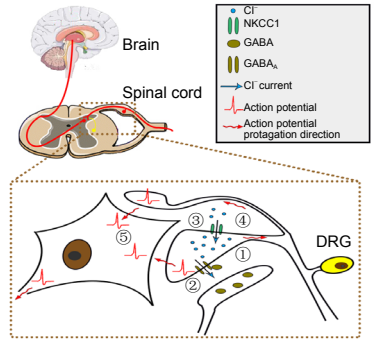

Figure 10 Hypothetical mechanism by which NKCC1 leads to increased excitability of DRG neurons and consequent neuropathic pain.
① In the central nerve terminal of the DRG neurons, the concentration gradient causes Cl^- outflow, and GABA mediates primary afferent depolarization (Carlton, 2014). ② The intensity of the primary afferent depolarization is affected by the concentration gradient of Cl^-. The higher the Cl^- concentration in DRG neurons, the stronger the primary afferent depolarization. Once primary afferent depolarization reaches the threshold of the nerve endings, it induces dorsal root reflex responses (Willis, 1999). ③ Increased expression of NKCC1 in neuropathic pain leads to an influx of Cl- into DRG neurons and an enhanced concentration gradient of Cl^-. Primary afferent depolarization is enhanced and the dorsal root reflex is more easily produced. ④ Action potentials caused by the dorsal root reflex can be transmitted to other central nerve terminals of DRG neurons. ⑤ Action potentials travel along fibers to the central nerve terminals of the DRG and then to the neurons in the dorsal spinal cord. NKCC1: Na^+-K^+-$2Cl^-$ cotransporter; DRG: dorsal root ganglion.

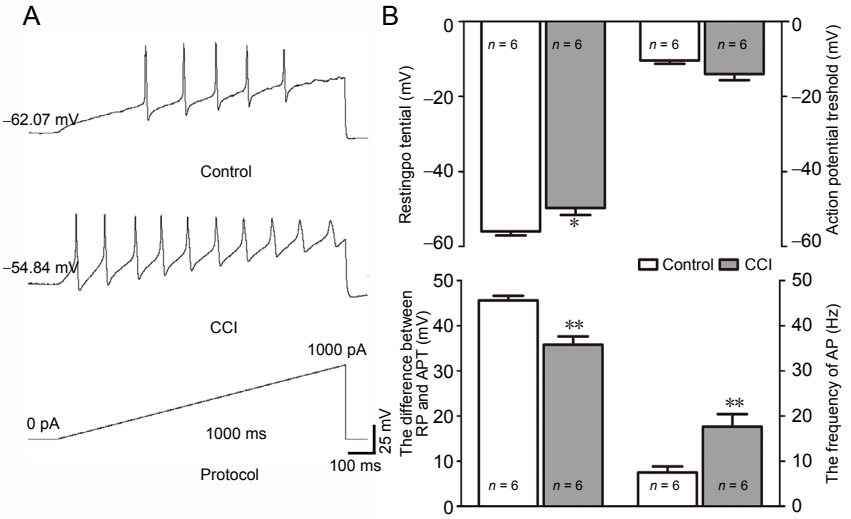

Figure 7 Changes in action potentials of dorsal root ganglion neurons in rats.
(A) Action potentials of dorsal root ganglion neurons in the control and CCI rats. (B) Difference between RP and APT, and frequency of action potential of DRG neurons in saline control and CCI rats. *P < 0.05, **P < 0.01, *vs.* control group. Data are expressed as the mean ± SEM (n = 6; independent-sample t-test). APT: Action potential threshold; CCI: chronic constriction injury; RP: resting potential.

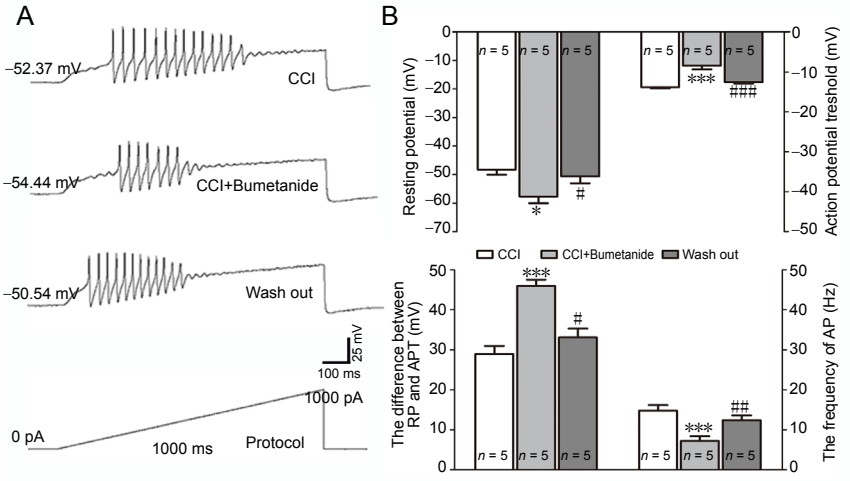

Figure 8 Effect of bumetanide on action potentials activated by ramp stimulation of dorsal root ganglion neurons.
(A) Action potentials of dorsal root ganglion neurons with and without bumetanide in CCI rats. (B) Difference between RP and APT, and frequency of action potential of DRG neurons in CCI, CCI + bumetanide, and washed-out DRG neuron groups. *P < 0.05, ***P < 0.001, *vs.* CCI group; #P < 0.05, ##P < 0.01, ###P < 0.001, *vs.* CCI + bumetanide group. Data are expressed as the mean ± SEM (n = 5; one-way analysis of variance followed by Tukey's *post hoc* test). APT: Action potential threshold; CCI: chronic constriction injury; RP: resting potential.

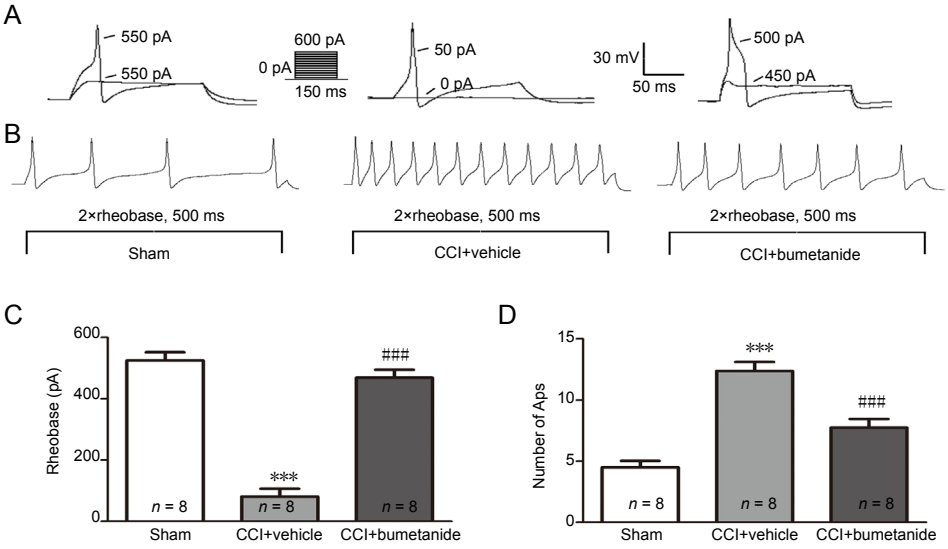

Figure 9 Effect of bumetanide on action potentials activated by step stimulation of dorsal root ganglion neurons.

(A) Rheobase of dorsal root ganglion neurons with and without bumetanide in CCI rats. (B) Action potentials elicited by a depolarizing current (500 ms) at twice the strength of the rheobase in each group. (C) Rheobase of action potentials in each group. (D) Numbers of action potentials in each group. ***P < 0.001, *vs.* sham group; ###P < 0.001, *vs.* CCI + vehicle group. Data are expressed as the mean ± SEM (n = 5; one-way analysis of variance followed by Tukey's *post hoc* test). CCI: Chronic constriction injury.

Janssen SP, Truin M, Van Kleef M, Joosten EA (2011) Differential GABAergic disinhibition during the development of painful peripheral neuropathy. Neuroscience 184:183-194.

Lamas JA, Fernández-Fernández D (2019) Tandem pore TWIK-related potassium channels and neuroprotection. Neural Regen Res 14:1293-1308.

Li L, Zhao L, Wang Y, Ma KT, Shi WY, Wang YZ, Si JQ (2015) PKCvarepsilon mediates substance P inhibition of GABAA receptors-mediated current in rat dorsal root ganglion. J Huazhong Univ Sci Technolog Med Sci 35:1-9.

Miletic G, Miletic V (2008) Loose ligation of the sciatic nerve is associated with TrkB receptor-dependent decreases in KCC2 protein levels in the ipsilateral spinal dorsal horn. Pain 137:532-539.

Modol L, Cobianchi S, Navarro X (2014) Prevention of NKCC1 phosphorylation avoids downregulation of KCC2 in central sensory pathways and reduces neuropathic pain after peripheral nerve injury. Pain 155:1577-1590.

Modol L, Santos D, Cobianchi S (2015) NKCC1 Activation is required for myelinated sensory neurons regeneration through JNK-dependent pathway. J Neurosci 35:7414-7427.

Morales-Aza BM, Chillingworth NL, Payne JA, Donaldson LF (2004) Inflammation alters cation chloride cotransporter expression in sensory neurons. Neurobiol Dis 17:62-69.

Munro G, Erichsen HK, Rae MG, Mirza NR (2011) A question of balance--positive versus negative allosteric modulation of GABA(A) receptor subtypes as a driver of analgesic efficacy in rat models of inflammatory and neuropathic pain. Neuropharmacology 61:121-132.

Payne JA, Stevenson TJ, Donaldson LF (1996) Molecular characterization of a putative K-Cl cotransporter in rat brain. A neuronal-specific isoform. J Biol Chem 271:16245-16252.

Payne JA, Rivera C, Voipio J, Kaila K (2003) Cation-chloride co-transporters in neuronal communication, development and trauma. Trends Neurosci 26:199-206.

Plotkin MD, Kaplan MR, Peterson LN, Gullans SR, Hebert SC, Delpire E (1997) Expression of the Na(+)-K(+)-2Cl- cotransporter BSC2 in the nervous system. Am J Physiol 272:C173-183.

Price TJ, Cervero F, de Koninck Y (2005) Role of cation-chloride-cotransporters (CCC) in pain and hyperalgesia. Curr Top Med Chem 5:547-555.

Price TJ, Cervero F, Gold MS, Hammond DL, Prescott SA (2009) Chloride regulation in the pain pathway. Brain Res 60:149-170.

Rau KK, Caudle RM, Cooper BY, Johnson RD (2005) Diverse immunocytochemical expression of opioid receptors in electrophysiologically defined cells of rat dorsal root ganglia. J Chem Neuroanat 29:255-264.

Rivera C, Voipio J, Payne JA, Ruusuvuori E, Lahtinen H, Lamsa K, Pirvola U, Saarma M, Kaila K (1999) The K^+/Cl^- co-transporter KCC2 renders GABA hyperpolarizing during neuronal maturation. Nature 397:251-255.

Samuel WC, Christopher B, John C, Jessica T, Bradley A, Gurwattan M, Sharad R, Dandan S, Daniel R (2008) The role of cation-dependent chloride transporters in neuropathic pain following spinal cord injury. Mol Pain 4:1-8.

Sung KW, Kirby M, McDonald MP, Lovinger DM, Delpire E (2000) Abnormal GABAA receptor-mediated currents in dorsal root ganglion neurons isolated from Na-K-2Cl cotransporter null mice. J Neurosci 20:7531-7538.

Trapp LD (2006) Mechanisms of acute pain: an update. J Calif Dent Assoc 34:955-958.

Walcott EC, Langdon RB (2002) Synaptically driven spikes and long-term potentiation in neocortical layer 2/3. Neuroscience 112:815-826.

Wang LJ, Wang Y, Chen MJ, Tian ZP, Lu BH, Mao KT, Zhang L, Zhao L, Shan LY, Li L, Si JQ (2017) Effects of niflumic acid on gamma-aminobutyric acid-induced currents in isolated dorsal root ganglion neurons of neuropathic pain rats. Exp Ther Med 14:1373-1380.

Wang XB, Li LY (2019) Interaction between satellite glial cells and neurons in sensory neuropathic pain. Zhongguo Zuzhi Gongcheng Yanjiu 23:1788-1793.

Willis WD Jr. (1999) Dorsal root potentials and dorsal root reflexes: a double-edged sword. Exper Brain Res 124:395-421.

Yousuf MS, Zubkow K, Tenorio G, Kerr B (2017) The chloride co-transporters, NKCC1 and KCC2, in experimental autoimmune encephalomyelitis (EAE). Neuroscience 344:178-186.

Zheng JH, Walters ET, Song XJ (2007) Dissociation of dorsal root ganglion neurons induces hyperexcitability that is maintained by increased responsiveness to cAMP and cGMP. J Neurophysiol 97:15-25.

P-Reviewers: Christensen B, Colonna MR, Ronchi G; C-Editor: Zhao M; S-Editors: Wang J, Li CH; L-Editors: Cason N, Robens J, Qiu Y, Song LP; T-Editor: Jia Y